

**SYNTHESIS, CHARACTERIZATION AND  
PHOTOCATALYTIC ACTIVITY OF GO/ZnO/Ag  
COMPOSITE FOR THE IMIDACLOPRID  
DEGRADATION**

**SAIMA KHAN AFRIDI**

**UNIVERSITI SAINS MALAYSIA**

**2025**

**SYNTHESIS, CHARACTERIZATION AND  
PHOTOCATALYTIC ACTIVITY OF GO/ZnO/Ag  
COMPOSITE FOR THE IMIDACLOPRID  
DEGRADATION**

by

**SAIMA KHAN AFRIDI**

**Thesis submitted in fulfilment of the requirements  
for the degree of  
Master of Science**

**June 2025**

## ACKNOWLEDGEMENT

I express my gratitude and admiration to almighty Allah for His blessings and benevolence in granting me the opportunity to commence and successfully finish the master's degree curriculum. I would like to express my sincere appreciation and respect to my supervisor, Asst. Prof. Dr. Khalid Umar, co-supervisor, Dr. Nur Farhana Jaafar, laboratory staff, and colleagues especially Dr. Hayfa Alajilani who have greatly contributed to the success and fulfilment of my academic journey at Universiti Sains Malaysia (USM). The guidance and support provided by my supervisor significantly contributed to the successful outcome of the project. I am grateful to my colleagues and school staff from the School of Chemical Sciences for their assistance and direction at various stages of the research endeavour.

My success was due to my parents, Mohd Fareed Khan and Arifa Khan, who encouraged and loved me. Their support inspired me to succeed and pursue my passion. I also appreciate my siblings Dr. Nida Fatima and Er. Mohd Aamir Khan's support. Thanks to Dr. Tabassum Parveen for being my second family while I was abroad and always supporting me. I am grateful to Husn Ara Chauhan for her unwavering support. My friends Aseel Yaghi, Hanadi Ahmad, Naseem Akhtar, Samia Awan, Sayyeda Farha, and others. I also appreciate Universiti Sains Malaysia's short-term grant (304/PKIMIA/6315580). Finally, I would like to thank the Malaysian Technical Cooperation Programme (MTCP), under the Ministry of Foreign Affairs, Malaysia, for providing me with a generous scholarship to support my Master's journey and allow me to connect with international scholars.

## TABLE OF CONTENTS

<b>ACKNOWLEDGEMENT</b> .....	<b>ii</b>
<b>TABLE OF CONTENTS</b> .....	<b>iii</b>
<b>LIST OF TABLES</b> .....	<b>vii</b>
<b>LIST OF FIGURES</b> .....	<b>viii</b>
<b>LIST OF ABBREVIATIONS</b> .....	<b>xi</b>
<b>ABSTRAK</b> .....	<b>xiv</b>
<b>ABSTRACT</b> .....	<b>xvi</b>
<b>CHAPTER 1 INTRODUCTION</b> .....	<b>1</b>
1.1 Research background .....	1
1.2 Problem statement.....	6
1.3 Research objectives.....	7
1.4 Scope of research .....	8
<b>CHAPTER 2 LITERATURE REVIEW</b> .....	<b>11</b>
2.1 Water Contamination .....	11
2.2 Pesticides .....	11
2.2.1 Adverse effects of pesticides.....	12
2.2.2 Systematic classification of pesticides.....	15
2.3 Organic pollutant: Imidacloprid.....	19
2.3.1 Previously reported photocatalysts for Imidacloprid degradation.....	21
2.4 Various bio precursors for graphene derivatives synthesis .....	24
2.4.1 Rice Husk.....	24
2.4.2 Oil Palm Waste.....	25
2.4.3 Lignin Waste .....	25
2.4.4 Chitosan .....	26
2.4.5 Sugarcane Bagasse .....	26

2.4.6	Wheat Straw .....	26
2.4.7	Green synthesis of ZnO using Citrullus lanatus .....	27
2.5	Photocatalysis/ Photocatalytic degradation .....	30
2.5.1	Need for Photocatalytic Degradation.....	31
2.5.2	Advantages of Photodegradation.....	31
2.5.3	Mechanism of Photodegradation.....	32
2.5.4	Semiconductor photocatalysts.....	33
2.5.5	Semiconductor photocatalysis.....	35
2.5.6	Synergistic Effects Enhancing GO/ZnO/Ag Photocatalysis .....	36
2.6	GO, ZnO, Ag and its composites as photocatalysts .....	38
2.6.1	Degradation of Pollutants by GO/ZnO Composite .....	38
2.6.2	Degradation of Pollutants by GO/ZnO/Ag Composite.....	41
2.7	Summary.....	44
<b>CHAPTER 3 METHODOLOGY.....</b>		<b>45</b>
3.1	Introduction.....	45
3.1.1	Experimental flowchart.....	46
3.2	Raw materials, chemicals and instruments.....	47
3.2.1	Raw materials and chemicals .....	47
3.2.2	Instruments.....	48
3.3	Synthesis of Graphene oxide, ZnO and its nanocomposite .....	49
3.3.1	Preparation of Oil Palm Empty Fruit Bunch (OPEFB) derived graphite powder .....	49
3.3.2	Synthesis of Graphene Oxide (GO).....	50
3.3.3	Green synthesis of ZnO .....	52
3.3.4	Synthesis of GO/ZnO .....	53
3.3.5	Synthesis of graphene oxide-zinc oxide-silver (GO/ZnO/Ag) nanocomposite.....	53
3.4	Characterization of GO, ZnO, GO/ZnO and GO/ZnO/Ag .....	54

3.4.1	Fourier transform infrared spectroscopy (FTIR) analysis .....	55
3.4.2	X-ray diffractometry (XRD) analysis .....	55
3.4.3	Raman analysis.....	55
3.4.4	Ultraviolet-visible diffuse reflectance spectroscopy (UV-DRS) analysis.....	56
3.4.5	Photoluminescence (PL) analysis.....	56
3.4.6	Scanning electron microscope (SEM) and Energy dispersive X-ray (EDX) analysis .....	56
3.4.7	Transmission electron microscope (TEM) analysis .....	57
3.4.8	Brunauer-Emmett-Teller (BET) analysis.....	57
3.4.9	Point of Zero Charge (PZC).....	58
3.5	Photocatalytic degradation of imidacloprid pesticide .....	58
3.5.1	Irradiation time .....	60
3.5.2	Initial concentration .....	60
3.5.3	Catalyst loading .....	60
3.5.4	Medium pH .....	61
3.6	Reusability test.....	61
3.7	Reaction kinetics .....	62
3.8	Scavenger test .....	63
3.8.1	Gas Chromatography-Mass Spectroscopy (GC-MS) .....	63
<b>CHAPTER 4 RESULTS AND DISCUSSION .....</b>		<b>65</b>
4.1	Introduction.....	65
4.2	Characterization of nanocomposites .....	65
4.2.1	Scanning electron microscope (SEM)/ Energy dispersive X-ray (EDX).....	65
4.2.2	Transmission electron microscope (TEM).....	71
4.2.3	X-ray diffractometry (XRD) analysis .....	73
4.2.4	Fourier transform infrared spectroscopy (FTIR).....	76
4.2.5	Ultraviolet-visible diffuse reflectance spectroscopy (UV-DRS) .....	79

4.2.6	Photoluminescence (PL) .....	82
4.2.7	Raman analysis .....	83
4.2.8	Brunauer-Emmett-Teller (BET) analysis .....	85
4.2.9	Point of Zero Charge (PZC) .....	88
4.3	Photocatalytic Experiment .....	90
4.4	Photocatalytic activity assessment .....	92
4.5	Study of photocatalytic degradation parameters .....	96
4.5.1	Effect of irradiation time .....	96
4.5.2	Effect of Imidacloprid concentration .....	97
4.5.3	Effect of GO/ZnO/Ag dosage .....	98
4.5.4	Effect of pH .....	100
4.6	Reusability of the photocatalyst .....	102
4.7	Reaction kinetics .....	103
4.8	Scavenger test .....	104
4.9	Photocatalytic degradation pathway of Imidacloprid using GO/ZnO/Ag nanocomposite .....	106
<b>CHAPTER 5 CONCLUSION AND FUTURE RECOMMENDATIONS .....</b>		<b>109</b>
5.1	Conclusion .....	109
5.2	Future research recommendations .....	110
<b>REFERENCES .....</b>		<b>112</b>
<b>LIST OF PUBLICATIONS</b>		

## LIST OF TABLES

	<b>Page</b>
Table 2.1	Pesticides impact routes on human health. .... 12
Table 2.2	Pesticide classification on the basis of commercial forms ..... 16
Table 2.3	Pesticide classification based on targeted pest species ..... 17
Table 2.4	Pesticides classification on the basis of persistency..... 18
Table 2.5	Classification based on the World Health Organization's guidelines for pesticide toxicity (WHO). ..... 18
Table 2.6	Summary of key studies on photocatalytic degradation of Imidacloprid using nanocomposites..... 24
Table 2.7	Photocatalysts similar to this research for the photodegradation of a variety of pollutants ..... 43
Table 3.1	List of raw materials and chemicals ..... 47
Table 3.2	List of instruments..... 48
Table 4.1	Specific surface area, pore volume and pore width of nanocomposites GO/ZnO/Ag, GO/ZnO, synthesized ZnO, and commercial ZnO. .... 87
Table 4.2	Rate constant and Regression coefficient values for Imidacloprid degradation under optimal degradation parameters..... 104

## LIST OF FIGURES

	<b>Page</b>
Figure 1.1	Graphene oxide (GO) structure showing $sp^2$ and $sp^3$ domains.....5
Figure 2.1	Diseases caused by the ingress of pesticides in human body through oral, dermal and respiratory routes..... 12
Figure 2.2	Worldwide pesticide consumption from 2023-2027 (FAO, 2023)..... 13
Figure 2.3	Annual death rate in the United States from the year 2000 to 2017 due to exposure to several pesticides (CDC, 2024)..... 14
Figure 2.4	The Environmental Performance Index for pesticide pollution risk (2024) in 180 different countries (EPI, 2024)..... 14
Figure 2.5	Classification of Pesticides (Ansari et al., 2021) (Hassaan & El Nemr, 2020) (Alengebawy et al., 2021)..... 16
Figure 2.6	Molecular structures of most common pesticides..... 19
Figure 2.7	Chemical structure of Imidacloprid (IMD).....21
Figure 2.8	Advantages of Photodegradation.....32
Figure 2.9	Mechanism of Photocatalytic Degradation.....33
Figure 2.10	Various categories of semiconductor photocatalysts.....34
Figure 2.11	Few examples of various dopants in conjunction with semiconductor-based nanocomposites for organic pollutant degradation.....36
Figure 2.12	Advantages of doped photocatalyst.....38
Figure 2.13	Illustration of ZnO/GO nanocomposite synthesis and mechanism of photodegradation under UV-Light.....40
Figure 3.1	Experimental flowchart for the degradation of IMD by photocatalysis under UV-Visible light.....46
Figure 3.2	Carbonization process of OPEFB.....50
Figure 3.3	Steps involved in graphene oxide (GO) synthesis using modified Hummer's method.....51
Figure 3.4	Steps involved in green synthesis of zinc oxide (ZnO).....53

Figure 4.1	The SEM image of (a) GO at 50.0k magnification (b) EDX spectrum of GO. ....	66
Figure 4.2	The SEM image of (a) green synthesized ZnO at 50.0k magnification (b) EDX spectrum of ZnO (c) particle size distribution of ZnO photocatalyst. ....	67
Figure 4.3	The SEM image of (a) commercial ZnO at 30.0k magnification (b) EDX spectrum of ZnO (c) particle size distribution of ZnO photocatalyst. ....	68
Figure 4.4	The SEM image of (a) synthesized GO/ZnO at 30.0k magnification (b) EDX spectrum of GO/ZnO (c) particle size distribution of GO/ZnO photocatalyst. ....	69
Figure 4.5	The SEM image of (a) synthesized GO/ZnO/Ag at 30.0k magnification (b) EDX spectrum of GO/ZnO/Ag (c) particle size distribution of GO/ZnO/Ag photocatalyst. ....	70
Figure 4.6	TEM image illustration of Graphene oxide (GO) structure. ....	72
Figure 4.7	TEM image illustration of commercial ZnO nanoparticles. ....	72
Figure 4.8	TEM image illustration of synthesized ZnO nanoparticles. ....	72
Figure 4.9	TEM image illustration of synthesized GO/ZnO nanoparticles. ....	73
Figure 4.10	TEM image illustration of synthesized GO/ZnO/Ag nanoparticles. ....	73
Figure 4.11	XRD analysis of commercial ZnO, synthesized ZnO, GO, GO/ZnO, and GO/ZnO/Ag nanocomposite. ....	75
Figure 4.12	FTIR spectra of commercial ZnO, synthesized ZnO, GO, GO/ZnO, and GO/ZnO–Ag nanocomposite. ....	77
Figure 4.13	UV-Visible DRS spectroscopy analysis of commercial ZnO, synthesized ZnO, GO/ZnO and GO/ZnO/Ag nanocomposites. ....	80
Figure 4.14	Tauc plot to determine the optical band gap of commercial ZnO, synthesized ZnO, and GO/ZnO nanocomposites. ....	81
Figure 4.15	PL spectra of the commercial ZnO, synthesised ZnO, GO/ZnO, and GO/ZnO/Ag nanocomposites. ....	83
Figure 4.16	(a) Raman Spectrum of GO, GO/ZnO and GO/ZnO/Ag nanocomposites in the range of 1000-2000 $\text{cm}^{-1}$ and (b) Raman Spectrum of synthesized and commercial ZnO nanoparticles in the range 300-600 $\text{cm}^{-1}$ . ....	85

Figure 4.17	Type IV N <sub>2</sub> adsorption-desorption isotherm with H <sub>3</sub> hysteresis loop for the BET surface area analysis and corresponding pore size distribution (inset) of (a) GO/ZnO/Ag nanocomposite, (b) GO/ZnO nanocomposite, (c) synthesized ZnO, and (d) commercial ZnO.....	86
Figure 4.18	Point of Zero Charge (pH <sub>PZC</sub> ) plot of GO/ZnO/Ag nanocomposite .....	90
Figure 4.19	Photocatalytic performances of various photocatalysts studied for the degradation of Imidacloprid. ....	91
Figure 4.20	Change in absorbance for the degradation of IMD in the presence of GO/ZnO/Ag photocatalyst. ....	92
Figure 4.21	Schematic mechanism of Imidacloprid photodegradation by GO/ZnO/Ag photocatalyst.....	95
Figure 4.22	Change in the concentration for the degradation of Imidacloprid over time in the presence of commercial ZnO, synthesized ZnO, GO/ZnO and GO/ZnO/Ag at 2 g/L concentration.....	97
Figure 4.23	Effect of pesticide concentration on the degradation of Imidacloprid.....	98
Figure 4.24	Effect of catalyst concentration on the degradation of Imidacloprid.....	99
Figure 4.25	Effect of pH on the degradation of Imidacloprid.....	101
Figure 4.26	Reusability analysis of GO/ZnO/Ag photocatalyst for the degradation of Imidacloprid. The irradiation duration of 1 cycle was 135 minutes.....	102
Figure 4.27	Linear curve fitting for pseudo first-order reaction kinetics model of Imidacloprid degradation under optimal degradation parameters.....	104
Figure 4.28	Effect of various scavengers (1mM) on the degradation of IMD (25 ppm) in the presence of GO/ZnO/Ag (2 g/L) photocatalyst.....	106
Figure 4.29	Total ion chromatograms of degraded Imidacloprid (a) at T = 0 hours, (b) at T = 4 hours, and (c) at T = 9 hours. (Concentration: 25 ppm; pH: 10, photocatalyst dose: 2g/L; UV-Visible light).....	107
Figure 4.30	Proposed degradation pathway and intermediate product formation for the degradation of Imidacloprid (25 ppm) using GO/ZnO/Ag (2 g/L) photocatalyst over the span of 9 hours.....	108

## LIST OF ABBREVIATIONS

2D	Two-Dimensional
Ag	silver
AgNO <sub>3</sub>	silver nitrate
AOP	Advance Oxidation Processes
BET	Brunauer-Emmett-Teller
BF	Basic Fuchsin
BJH	Barrett, Joyner, and Halenda
BN	Boron Nitride
CB	Conduction Band
CdS	Cadmium Sulfide
CF	Ciprofloxacin
CO <sub>2</sub>	Carbon dioxide
CR	Congo red
CV	Crystal Violet
EC	European Community
EDTA-2Na	Ethylenediaminetetraacetic Acid Disodium
EDX	Energy dispersive X-ray
E <sub>g</sub>	Band Gap energy
FLG	Few Layer Graphene
FTIR	Fourier Transform Infrared Spectroscopy
GaAs	Gallium Arsenide
GaN	Gallium Nitride
GC-MS	Gas Chromatography-Mass Spectroscopy
GO	Graphene Oxide
GV	Granulosis Virus

$h^+$	positive holes
$H_2O$	chemical formula for water
$h\nu$	photon energy
IMD	Imidacloprid
IPA	Isopropyl Alcohol
KBr	Potassium bromide
LEVO	Levofloxacin
LSPR	Localised Surface Plasmon Resonance
MO	Methyl Orange
MR	Methyl Red
NC	Nanocellulose
NEO-Is	Neonicotinoid Insecticides
ng/L	nanograms per litre
NPV	Nuclear polyhedrosis virus
NR	Neutral Red
$\cdot O_2^-$	superoxide anions
$\cdot OH$	hydroxyl radical
OP	Organic Pollutants
OPEFB	Oil Palm Empty Fruit Bunch
OPP	Organophosphorus Pesticides
pH	measure of how acidic
$pH_i$	starting pH value
$pH_{PZC}$	surface charge is neutral
PL	Photoluminescence
ppb	parts per billion
ppm	parts per million
PZC	Point of Zero Charge

rGO	reduced Graphene Oxide
RhB	Rhodamine B
ROS	Reactive Oxygen Species
SAED	Selected Area Electron Diffraction
SEM	Scanning Electron Microscope
SERC	Science and Engineering Research Centre
SiC	Silicon Carbide
SPR	Surface Plasmon Resonance
TC	Tetracycline Hydrochloride
TEM	Transmission electron microscope
TiO <sub>2</sub>	Titanium Dioxide
TOC	Total Organic Carbon
trPL	Transient photoluminescent
UV	Ultraviolet
UV-DRS	Ultraviolet-Visible Diffuse Reflectance Spectroscopy
UV-Vis	UV-Visible spectroscopy
VB	Valence Band
WRE	Watermelon Rind Extract
XRD	X-ray Diffraction
ZnO	Zinc Oxide
ZnO-GO/NC	Zinc Oxide-Graphene Oxide/Nanocellulose
GO/ZnO	Graphene Oxide/ Zinc Oxide
GO/ZnO/Ag	Graphene Oxide/Zinc Oxide/Silver
ZnS	Zinc Sulfide
ΔpH	Variation in pH value
μg/L	micrograms per litre

# **SINTESIS, PENCIRIAN DAN AKTIVITI PEMFOTOMANGKIN KOMPOSIT GO/ZNO/AG UNTUK DEGRADASI IMIDACLOPRID**

## **ABSTRAK**

Dalam kajian ini, satu nanokomposit ternari (GO/ZnO/Ag) iaitu grafena oksida (GO) antara muka. fotomangkin zink oksida (ZnO), didop dengan dengan perak (Ag) telah disintesis untuk degradasi imidacloprid (IMD). Untuk sintesis GO, serat tandan buah kosong kelapa sawit (OPEFB) digunakan sebagai pendahulu untuk penyediaan grafit. Untuk sintesis hijau ZnO, ekstrak kulit tembikai (WRE) digunakan sebagai agen pengurangan. Nanokomposit yang disintesis dianalisis dengan spektroskopi inframerah transformasi Fourier (FTIR), spektroskopi pantulan cahaya UV-Vis (UV-Vis DRS), pembelauan sinar-X (XRD), mikroskopi elektron imbasan (SEM) dengan sinar-X hamburan tenaga (EDX), mikroskopi elektron transmisi (TEM), fotoluminesens (PL), analisis Raman, Brunauer-Emmett-Teller (BET) dan Titik Cas Sifar (PZC). Pencirian mengesahkan penggabungan Ag dan penyelangan GO dalam fotomangkin ZnO. Tenaga jurang jalur nanokomposit GO/ZnO/Ag yang dikira daripada spektrum UV-DRS ialah 2.96 eV yang mengesahkan aktiviti cahaya tampak fotomangkin. Pada pH 10, nanokomposit GO/ZnO/Ag menunjukkan keupayaan cemerlang untuk mendegradasi 25 ppm IMD (100% degradasi) dalam 135 minit di bawah pendedahan cahaya UV-Tampak, diikuti oleh GO/ZnO (88.93%), ZnO yang disintesis (75.63%), dan ZnO komersial (71.485%). Kawasan permukaan yang lebih tinggi bagi fotomangkin ternari (71.43 m<sup>2</sup>/g) memberikan penyerapan pencemar yang lebih besar, dan pengurangan jurang jalur, pengurangan kadar rekombinasi dan penyerapan cahaya yang beralih ke kawasan tampak, membolehkan nanokomposit GO/ZnO/Ag menggunakan cahaya tampak dengan lebih cekap dan mempercepatkan

degradasi IMD. Reaksi fotodegradasi sesuai dengan model pseudo kinetik peringkat pertama dengan pekali regresi ( $R^2$ ) sebanyak 0.9942 dan pemalar kadar ( $k_{app}$ ) sebanyak  $0.0382 \text{ min}^{-1}$ . Ujian perencat yang dijalankan menunjukkan bahawa radikal superoksida dan hidroksil adalah spesies oksigen reaktif utama (ROS) yang terlibat dalam degradasi pemfotomangkin. Produk hasil sampingan yang lebih kecil seperti 2-kloro-5- metilpiridin (7;  $m/z = 126.5$ ) dan imidazolidin-2-one (8;  $m/z = 86$ ) yang dikenal pasti dalam GC-MS, dengan jelas menunjukkan pengujaan elektron dari fotomangkin yang disertakan diikuti oleh tindakan  $\cdot\text{O}_2^-$  dan  $\cdot\text{OH}$  (spesies aktif) berdasarkan pengoksidaan berasaskanimidaclopid. Selain itu, komposit yang disintesis menunjukkan kestabilan dan kebolehulangan, kerana kecekapan degradasinya hanya berkurang sebanyak 4.8% selepas empat kitaran berturut-turut. Oleh itu, nanokomposit GO/ZnO/Ag mempunyai potensi untuk menjadi fotomangkin fleksibel yang berkesan untuk menguraikan IMD dalam proses rawatan air sisa.

**SYNTHESIS, CHARACTERIZATION AND PHOTOCATALYTIC  
ACTIVITY OF GO/ZnO/Ag COMPOSITE FOR THE IMIDACLOPRID  
DEGRADATION**

**ABSTRACT**

In this study, a ternary nanocomposite (GO/ZnO/Ag) i.e., a graphene oxide (GO) interfaced, zinc oxide (ZnO) photocatalyst, doped with silver (Ag) is synthesized for imidacloprid (IMD) degradation. For GO synthesis, Oil Palm Empty Fruit Bunch Fiber (OPEFB) was used as its precursor for graphite preparation. For green synthesis of ZnO, watermelon rind extract (WRE) was used as a reducing agent. The as synthesized nanocomposites were analysed by Fourier transform infrared (FTIR) spectroscopy, UV-Visible diffuse reflectance spectroscopy (UV-Vis DRS), X-ray diffraction (XRD), Scanning electron microscopy (SEM) with Energy dispersive X-ray (EDX), Transmission electron microscopy (TEM), and Photoluminescence (PL), Raman analysis, Brunauer-Emmett-Teller (BET) and Point of Zero Charge (PZC). The characterizations confirmed the incorporation of Ag and interfacing of GO in the ZnO photocatalyst. The band gap energy of GO/ZnO/Ag nanocomposite calculated from the UV-DRS spectrum is 2.96 eV that confirms the visible light activity of the photocatalyst. At 10 pH, the GO/ZnO/Ag nanocomposite showed excellent ability to degrade 25 ppm of IMD (100% degradation) in 135 minutes under UV-Visible light exposure followed by GO/ZnO (88.93%), synthesized ZnO (75.63%), and commercial ZnO (71.485). The higher surface area of the ternary photocatalyst (71.43 m<sup>2</sup>/g) provided greater pollutant absorption, and the reduced bandgap, decreased recombination rate, and the light absorption shifted into the visible region, allowed the

GO/ZnO/Ag nanocomposite to utilise visible light more efficiently and accelerate the degradation of IMD. The photodegradation reaction fitted well with pseudo first-order kinetics model with a regression coefficient ( $R^2$ ) as 0.9942 a rate constant ( $k_{app}$ ) of  $0.0382 \text{ min}^{-1}$ . The scavenger test conducted indicated that the superoxide and hydroxyl radicals are the main reactive oxygen species (ROS) involved in photocatalytic degradation. The smaller byproducts like 2-chloro-5-methylpyridine (7;  $m/z = 127.6$ ) and imidazolidin-2-one (8;  $m/z = 86.1$ ) identified in GC-MS, clearly demonstrated  $e^-$  excitement from incorporated photocatalyst followed by the action of  $^{\cdot}O_2^-$  and  $\cdot OH$  (active species) based oxidation of imidacloprid. Furthermore, the synthesised composite exhibits stability and reproducibility, as its degrading efficiency only reduced by 4.8% after four consecutive cycles. Therefore, the GO/ZnO/Ag nanocomposite has the potential to be a flexible photocatalyst for efficiently breaking down IMD in the process of treating wastewater.

## CHAPTER 1

### INTRODUCTION

#### 1.1 Research background

Water pollution, a serious global issue, is driven by untreated effluents from sources like pharmaceutical, hospital, and various manufacturing industries. These discharges contain harmful pollutants such as drugs, dyes, and pesticides, which contaminate water bodies, endangering human health and aquatic life (Intisar et al., 2023). One such pollutant is Imidacloprid (IMI), a prominent member of the neonicotinoid class of insecticides, is globally utilized for its high efficacy against a broad spectrum of insect pests in agriculture, horticulture, and domestic settings (Wang et al., 2020).

As one of the top ten global agrochemicals, its extensive application includes seed treatments, soil applications, and foliar sprays to protect various crops and manage pests like termites and fleas. However, the widespread use of IMI has led to significant environmental concerns. Studies indicate that only a small fraction (around 1%) of applied pesticides effectively targets pests, with the remainder dispersing into the environment. In water, persistence is high, with reported half-lives ranging from 28 to 1250 days, often exceeding 100 days (Gao et al., 2024). For mammals, IMI is classified as moderately toxic via acute oral exposure and having dermal toxicity (WHO/EPA Class II or III) and mutagenic nature. Toxicological data suggests it can cause damage to organs, particularly the nervous system and liver, upon single or repeated exposure.

Given these severe impacts, control and removal of these contaminants from water must be undertaken immediately. However, the toxic nature, high solubility, stability, and slow biodegradation of the complex organic pollutants make it extremely challenging to remove them from water (Ghanbari & Moradi, 2017). Various water purifying technologies have been developed over time to remove these effluents from wastewater. These methods encompassed physical approaches such as filtration, flocculation, membrane separation etc. Chemical procedures involved the use of flocculants, coagulants and ozonation etc. Fungal, anaerobic, and aerobic decolorization were among the biological techniques used (Lops et al., 2019). However, these techniques don't completely turn the contaminants into minerals, CO<sub>2</sub> etc. but rather move them from one phase to another (Anas et al., 2016). They also have certain drawbacks, like a reduced ability to remove organic pigments that are resistant to biodegradation and the requirement for further subsequent processing and a longer treatment period (Lops et al., 2019). Drawbacks of adsorption and coagulation procedures include the formation of toxic byproducts and proliferation of secondary contaminants (Mittal et al., 2014).

To address these shortcomings and achieve complete degradation of pollutants, recently, Advance Oxidation Processes (AOPs) have been combined with the standard procedures listed above or used independently to create an efficient way for treating wastewater. This method converts contaminants into harmless substances (Anas et al., 2016; Yoon et al., 2014; Ong et al., 2018). In recent decades, heterogeneous photocatalysis utilising semiconductors has garnered significant interest as an environmentally friendly and sustainable technology, within the AOP family, owing to its capability to tackle energy and environmental challenges. Heterogeneous photocatalysis is an advanced oxidation process (AOP) that produces a metal oxide

semiconductor as a photocatalyst (Ayub et al., 2020). However, it is important to note that earlier research has developed most photocatalysts that work under UV light. Quite recently, researchers have tried to develop those catalysts that degrade pollutants under visible light. This is because sunlight is a clean, abundant, safe, and economical energy source. Solar light photocatalysis is an advanced oxidation process that forms reactive oxygen species (ROS). ROS include superoxide ( $O_2^-$ ) and hydroxyl ( $\bullet OH$ ) radicals. These ROS break down organic pollutants into safer products ( $CO_2$  and  $H_2O$ ). Despite its promise, photocatalyst still suffers from low quantum yields and weak responses in the visible light region, which limits its widespread application. To break the bottleneck of this technology, highly efficient visible light receptive photocatalysts with high quantum yields are necessary (Biswas et al., 2019).

Among the various semiconductors explored to meet this need, recently, zinc oxide (ZnO) has been majorly studied as a semiconductor photocatalyst material due to its superior properties such as environmental abundance, thermal stability, non-toxic nature, tunable bandgap, cheap price, and UV-Light adsorption (Girija Shankar et al., 2021). When ZnO is chemically mixed with other substances, it can form a highly conductive material. This material has practical uses in the field of electronics (Dutta et al., 2021). Furthermore, ZnO possess exceptional photosensitivity as a result of their distinct characteristics, including a high intrinsic electron mobility of  $300\text{ cm}^2/\text{Vs}$  (far greater than  $TiO_2$  with  $0.1\text{--}4.0\text{ cm}^2/\text{Vs}$ ), broad band gap of  $3.37\text{ eV}$ , and a high exciton binding energy of  $60\text{ meV}$ . Based on multiple studies it has been determined that ZnO is a superior catalyst compared to titanium dioxide ( $TiO_2$ ). ZnO is increasingly being used as a substitute for  $TiO_2$  because of its efficient absorption of sunlight, making it one of the most often used photocatalysts (Saravanan et al., 2018; Kumar et al., 2014; Kumar et al., 2020). ZnO exhibits enhanced conductivity due to its ability to efficiently

transport both electrons and holes when subjected to external energy. The position of the  $VB_{ZnO}$  is lower than that of  $VB_{TiO_2}$  therefore the oxidation potential of hydroxyl radical generated by ZnO is higher than that of hydroxyl radical produced by  $TiO_2$  leading to better photocatalytic performance (Turkten & Bekbolet, 2020).

Despite these significant advantages, there are certain disadvantages to using pristine ZnO in photocatalysis, including: (i) its large band gap, which limits its use in the visible range (Ahmed et al., 2016), (ii) particle aggregation during photocatalytic reactions, which severely limits ZnO's photocatalytic activity on a large scale, and (iii) the quick recombination of the electron-hole pairs that are photogenerated. This leads to decrease in the quantum produce and the dissipation of energy (Kumar & Rao, 2014).

To mitigate these issues and harness ZnO's potential more effectively, researchers often combine it with other materials. A carbon-based substance with two-dimensional properties that has shown great promise in this regard is called graphene. Graphene is a monolayer of carbon atoms in a honeycomb crystal lattice with  $sp^2$  hybridization. Other derivatives of graphene include GO (Graphene Oxide) additionally rGO (reduced Graphene Oxide), also multilayer graphene (often including graphene platelets or graphene flakes) (Tiwari et al., 2018). Graphene and its derivatives have distinctive properties such as covalently bonded structure, greater electrical conductivity, a specific surface area, improved mechanical strength, reduced redox potential, and economical production cost (Sattar, 2019). Graphene oxide (GO), a derivative of graphene, possesses amphiphilic nature, and aqueous stability. GO contains carboxylic, hydroxyl, and epoxide groups on its edges and basal planes. It has widely been used at current times as a photocatalyst hybrid. This is because GO provides enhanced electron transfer, and its ability to accept electrons, thus enhancing

the recombination time. Additionally, the pollutant molecule's conjugation with the aromatic rings in GO creating  $\pi$ - $\pi$  interactions, particularly in the  $sp^2$  regions of GO, provides favorable adsorption properties that help boost the catalyst's performance, as shown in Figure 1.1. Additionally, the carboxylic acid functional groups in GO exhibit strong interactions with ZnO nanoparticles. This leads to significant ZnO adsorption on GO. Lastly, GO can introduce oxygen vacancies in the lattice of ZnO, which extends its responsiveness to visible light. These findings have been supported by studies referenced as (Ahmed et al., 2016; Pan et al., 2014).

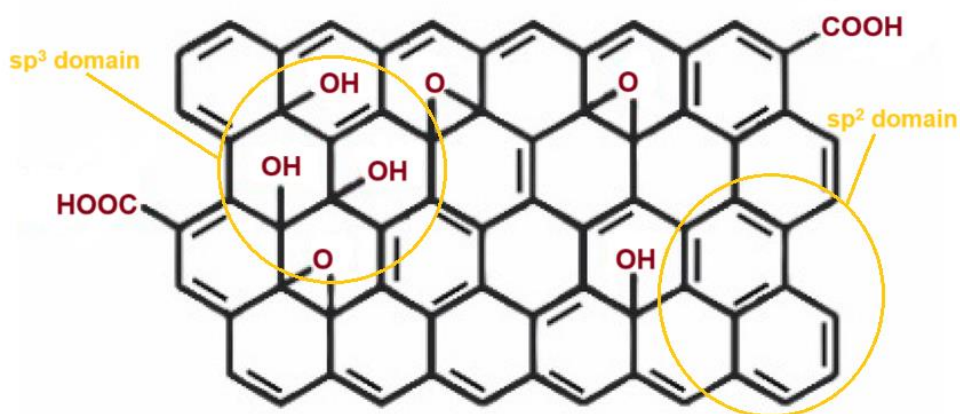


Figure 1.1 Graphene oxide (GO) structure showing  $sp^2$  and  $sp^3$  domains.

Besides combining ZnO with carbon materials, incorporating noble metals is another strategy to enhance photocatalysis. Owing to its notable characteristics, such as possessing antibacterial and catalytic properties, silver (Ag) metal is a compelling material to investigate at a nanoscale level. In addition, Ag also possesses unique surface plasmon resonance (SPR) and electron conductivity, which allows them to be used in photocatalysis. The presence of Ag nanoparticles enhances the absorption of light in the visible spectrum due to surface plasmon resonance (SPR). The presence of multiple unoccupied active sites makes it very suitable for the decomposition of

various dangerous contaminants (Kan et al., 2020). Nevertheless, the widespread utilisation of Ag nanoparticles is hindered by their tendency to combine and form agglomerates and clusters (Anees Ahmad et al., 2020). Therefore, integrating Ag within a composite structure like GO/ZnO offers several advantages, firstly, it mitigates the quick recombination of electron-hole pairs, and secondly, it prevents the aggregation of Ag, so maximising its potential in photocatalytic activity and lastly it enhances visible light response of GO/ZnO (Tran Thi et al., 2019).

Building upon the potential synergistic effects identified for GO, ZnO, and Ag, this study investigates the use of GO/ZnO/Ag nanoparticles in a photocatalytic process to eliminate imidacloprid from polluted water under UV-Visible irradiation.

## **1.2 Problem statement**

Water pollution from pesticides makes a major contribution to contamination due to the production of toxic chemicals that negatively impact the aquatic environment, human health, and the ecosystem (J. et al., 2020). One such pesticide is imidacloprid (IMD). The long-term exposure to IMD is linked to serious health problems in aquatic animals such as DNA disorders and embryotic disorders etc (Garrido et al., 2024; Vieira et al., 2018; Islam et al., 2019).

Semiconductor photocatalysis using materials like ZnO is a promising approach for pesticide degradation due to its efficiency and eco-friendliness (Opoku et al., 2017). However, pristine ZnO suffers from limitations, primarily the rapid recombination of photogenerated electron-hole pairs, which hinders its effectiveness. Modifications, such as doping, are necessary to overcome these drawbacks. Doping can mitigate recombination by widening the charge gap and trapping electrons, thereby enhancing photocatalytic efficiency compared to undoped ZnO, often due to

synergistic effects of altered band gap energy, increased surface area, and reduced particle size (Gnanasekaran et al., 2017).

This study investigates a GO/ZnO/Ag nanocomposite designed to improve charge carrier mobility and light absorption. Graphene oxide (GO) serves multiple roles: enhancing visible light absorption, acting as an electron conduit/acceptor to suppress recombination (Huang et al., 2017), preventing ZnO nanoparticle aggregation, improving pollutant adsorption via  $\pi$ - $\pi$  interactions, and potentially creating beneficial oxygen vacancies. Incorporating noble metals like silver (Ag) further stabilizes the photocatalyst. Ag nanoparticles act as electron traps via Schottky barriers, significantly reducing recombination and facilitating charge transfer. Additionally, Ag induces a Localized Surface Plasmon Resonance (LSPR) effect, boosting the generation of electron-hole pairs under illumination (Sescu et al., 2021; Ribao et al., 2019)

Furthermore, this work employed green synthesis methods. GO was synthesized from biomass waste (oil palm empty fruit bunch fibre), simultaneously valorising waste and producing a material suitable for photocatalytic applications. Similarly, ZnO was prepared using green techniques, minimizing chemical usage and toxicity compared to conventional methods, aligning with principles of sustainable chemistry (Safian et al., 2020). To our knowledge, OPEFB and WRE derived GO/ZnO/Ag nanocomposite has never been tested as a possible photocatalyst for pesticide degradation under UV-Visible light.

### **1.3 Research objectives**

The main objective of this research is to create photocatalyst by graphene oxide interfaced metal oxide and doped with noble metal nanocomposite. This photocatalytic

system will be used to effectively breakdown imidacloprid, a type of pesticide, when exposed to UV-Visible light. In order to accomplish this objective, three particular goals have been identified and addressed in the following manner:

- i) To synthesize GO from OPEFB (modified Hummer's method), green-synthesize ZnO using WRE, prepare GO/ZnO and GO/ZnO/Ag nanocomposites via facile solution-based method, and characterize all resulting materials.
- ii) To determine the photocatalytic activity and operational parameters (effect of imidacloprid concentration, GO/ZnO/Ag dosage, irradiation time and pH) of the synthesised photocatalyst (GO/ZnO/Ag) for pollutant degradation (imidacloprid pesticide) in aqueous medium.
- iii) To analyze the reaction kinetics, reusability, degradation mechanism and degradation pathway of the synthesised photocatalyst (GO/ZnO/Ag) for IMD degradation.

#### **1.4 Scope of research**

Photocatalysis methods utilising nanocomposites are becoming increasingly popular due to their wide range of applications in the environmental field. Also, photocatalysis using nanocomposites is an environmentally friendly and sustainable method for pollutant degradation, as it relies on UV-Visible or solar energy and does not require additional chemicals. The ability to utilise the immense potential of photoactive nanoparticles and gain access to their capabilities relies on the capacity to integrate them into photoreactors and effectively disperse them over large surfaces. In order to create nanocomposite materials that can be easily processed, it is essential to

include nanoparticles into suitable host substrates prior to integrating them into functional structures and, ultimately, products. The paper extensively examines the production of photocatalytic nanocomposite materials and their application in the destruction of persistent organic pollutants. Our focus is on modern methods for creating photocatalysts that are active under UV and visible light, as well as the process of modifying their surfaces after synthesis. Additionally, we explore how to incorporate the synthesised material into a suitable host matrix to create photocatalytic nanocomposites.

This research's scope focuses on synthesising ZnO photocatalyst utilising environmentally sustainable green synthesis method by using the watermelon rind extract (WRE) as a reducing and capping agent. In addition, graphene oxide (GO) was synthesised from graphitised oil palm empty fruit bunch (OPEFB) fibre using modified Hummer's method. The generated graphene oxide (GO) was interfaced with zinc oxide (ZnO) and doped with silver (Ag) nanoparticles derived from silver nitrate ( $\text{AgNO}_3$ ) using a facile solution-based synthesis method to create a nanocomposite known as GO/ZnO/Ag. Afterwards, the surface morphology and physicochemical properties of the photocatalysts were assessed utilising a range of characterization techniques such as Fourier transform infrared (FTIR) spectroscopy, X-ray diffractometry (XRD), Raman analysis, Ultraviolet-visible diffuse reflectance spectroscopy (UV-DRS), Photoluminescence (PL), Scanning electron microscope (SEM) and Energy dispersive X-ray (EDX), Transmission electron microscope (TEM), and Brunauer-Emmett-Teller (BET). The photocatalytic degradation of the imidacloprid pesticide was evaluated by the produced photocatalysts under UV-Visible light and analysed using UV-Visible spectroscopy (UV-Vis) analysis. The study also investigates the impacts of many variables, such as concentration of IMD, catalytic dosage, pH and irradiation time.

These parameter studies have been conducted to ascertain the ideal degradation state, which is crucial for the practical implementation of photocatalytic processes. Reaction kinetics, reaction mechanism, degradation pathway and reusability qualities of the photocatalyst on the process of photocatalytic degradation of IMD further assist in better assessment of photocatalyst-pollutant interaction.

The novelty of this research study lies in the synergistic combination of the unique physicochemical properties of GO, ZnO, and Ag coupled with strategic doping and optimization of reaction conditions, pave the way for highly efficient and sustainable water treatment method. The wide array of characterization techniques discussed in this thesis, provides a deep understanding of the material's properties and the factors contributing to its enhanced photocatalytic activity. Previous research studies involving similar nanocomposite structures have not investigated the degradation of neonicotinoid pesticides to the extent explored in this study. Furthermore, existing literature focusing on imidacloprid (IMD) degradation typically reports either longer degradation times or incomplete removal efficiencies. To the best of author's knowledge, there is no study which accounts for the bio-facilitated synthesis of the novel ternary GO/ZnO/Ag nanocomposite using Oil Palm Empty Fruit Bunch Fiber (OPEFB) and *Citrullus lanatus* extract with complete photocatalytic degradation towards IMD in a time duration as less as 135 min, with good recyclability.

## **CHAPTER 2**

### **LITERATURE REVIEW**

#### **2.1 Water Contamination**

Water, a vital natural resource, faces significant pollution challenges due to 21st-century industrialization and agricultural development. This contamination poses severe human health risks, causing waterborne diseases (e.g., cholera, typhoid) and potential long-term effects like cancer and neurological disorders (WHO, 2023; US EPA, 2017). Access to clean water remains a key humanitarian goal. Contributors to water pollution include growing livestock farms and domestic sewage effluents, introducing both inorganic and organic pollutants. Such pollution harms aquatic ecosystems by killing organisms, reducing biodiversity, and disrupting the food chain (Malaj et al., 2014).

#### **2.2 Pesticides**

This study focuses on pesticides, chemicals used to control pests such as insects (insecticides), fungi (fungicides), and weeds (herbicides). Benefits include increased agricultural productivity, reduced crop losses, and lower food costs (Alengebawy et al., 2021).

However, pesticide use leads to environmental contamination (soil, air, water), toxic exposure for workers and consumers (Table 2.1), the development of pesticide resistance requiring stronger chemicals (Begum et al., 2017), and links to chronic health issues like brain damage and cardiovascular ailments (Kim et al., 2017) (Alengebawy et al., 2021; Majhi et al., 2018) (Fig 2.1). Pesticides enter water bodies via runoff, persisting long-term. They harm aquatic life, disrupt food chains, reduce

biodiversity (Mahmood et al., 2016), and can cause eutrophication (Liu et al., 2021). These compounds are often highly toxic, stable, and difficult to degrade (Thakur et al., 2019).

Table 2.1 Pesticides impact routes on human health.

Sr No.	Route	Explanation
1	Oral	Pesticide ingestion as a pollutant in food stuff or via water
2	Respiratory	Inhalation of unintentionally dispersed spray and/or dust particles
3	Dermal	Exposure to pesticides on the skin while handling

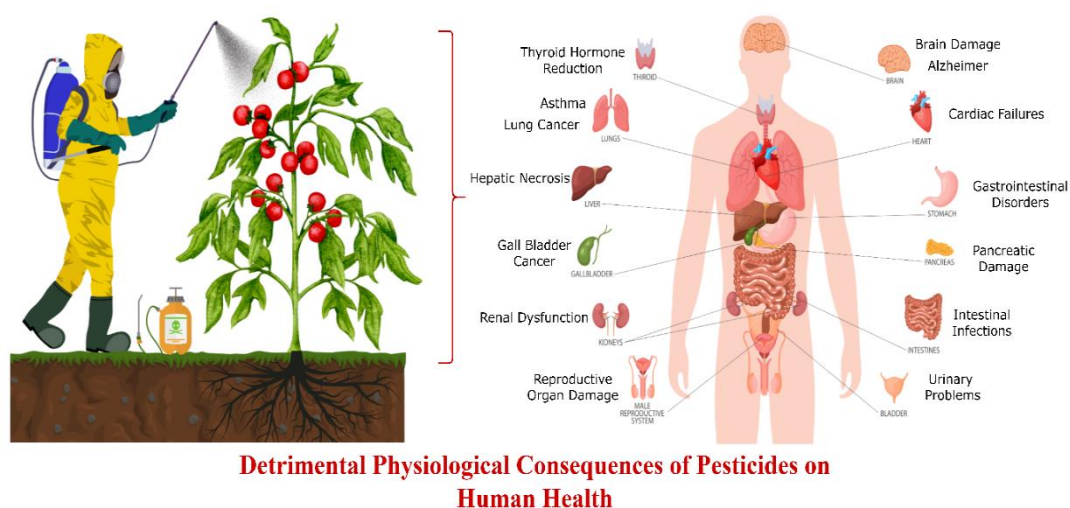


Figure 2.1 Diseases caused by the ingress of pesticides in human body through oral, dermal and respiratory routes.

### 2.2.1 Adverse effects of pesticides

Pesticides in water can act as potential mutagens, altering DNA (Hassaan & El Nemr, 2020). The WHO estimates around one million acute pesticide poisonings annually through direct contact, with mortality rates between 0.4% and 1.9% (Qiu et al., 2017; Eddleston, 2020; Jia et al., 2020). Global agricultural pesticide use is projected to slightly increase from about 4.3 million metric tonnes in 2023 to

approximately 4.41 million in 2027 (Fig 2.2) (FAO, 2023), with the Americas being the highest consuming region in 2021. US data reflects pesticide-related deaths (Fig 2.3) (CDC, 2024). The Environmental Performance Index (2024) ranked pesticide pollution risk for 180 countries, placing Malaysia fifth highest (Fig 2.4) (EPI, 2024). Addressing these effects necessitates effective water management strategies. European Community (EC) regulations limit total pesticides in drinking water to 0.5 g/L and individual pesticides to 0.1 g/L.

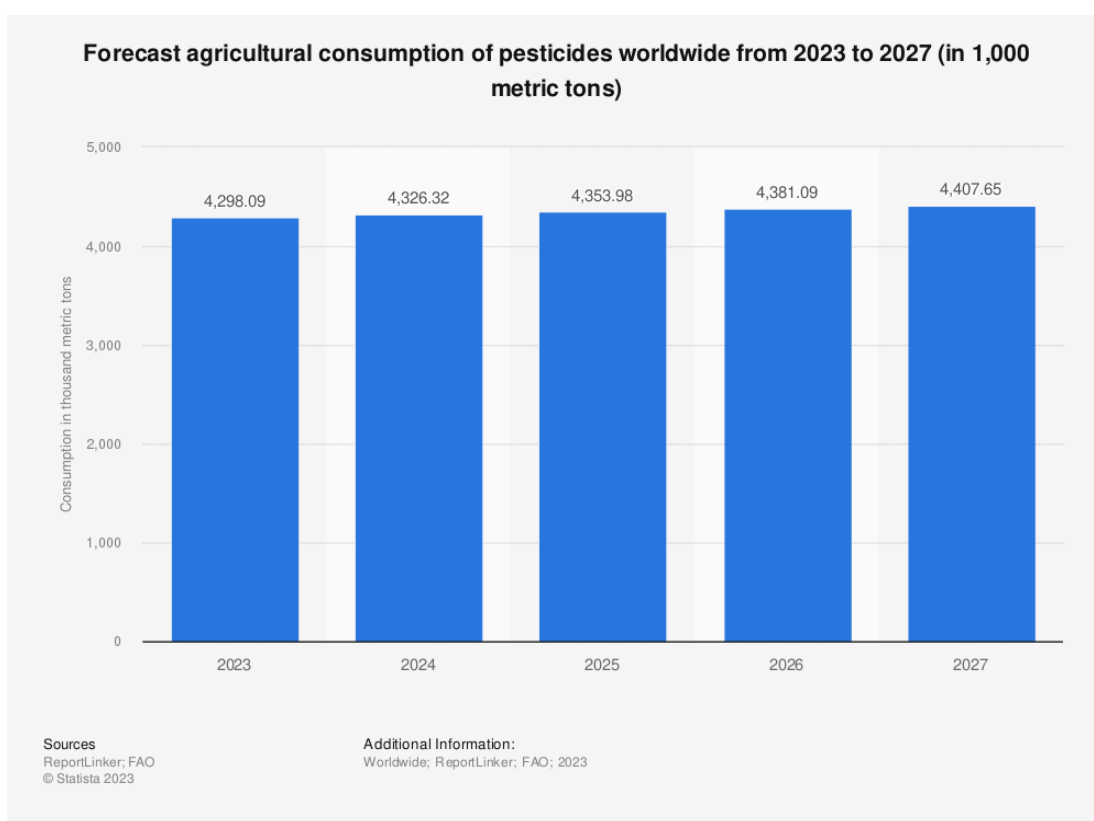


Figure 2.2 Worldwide pesticide consumption from 2023-2027 (FAO, 2023).

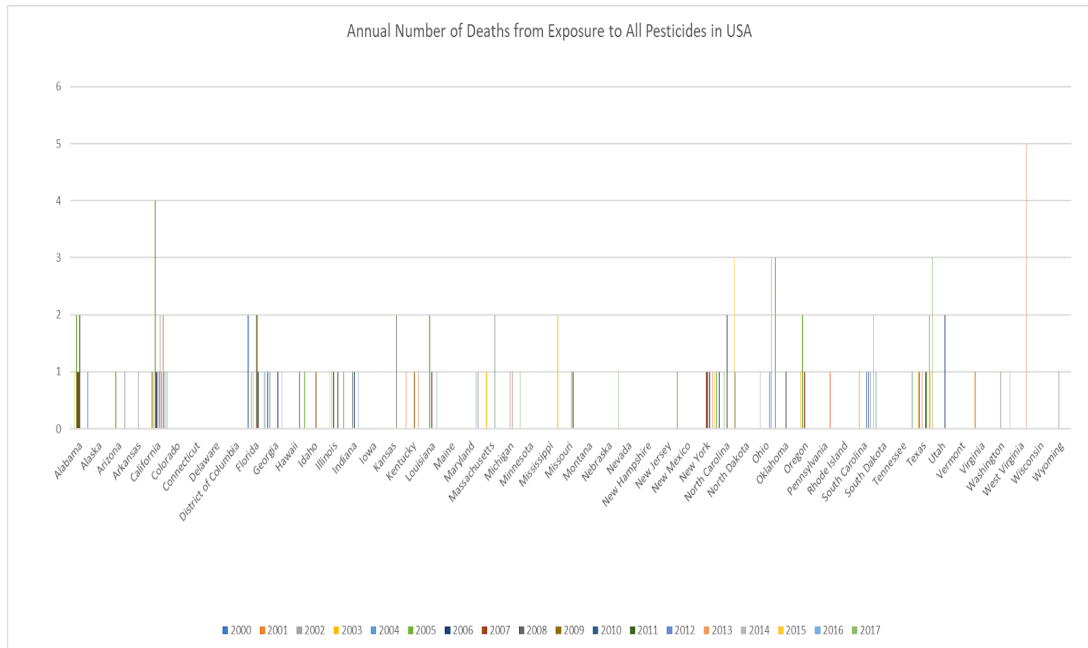


Figure 2.3 Annual death rate in the United States from the year 2000 to 2017 due to exposure to several pesticides (CDC, 2024).

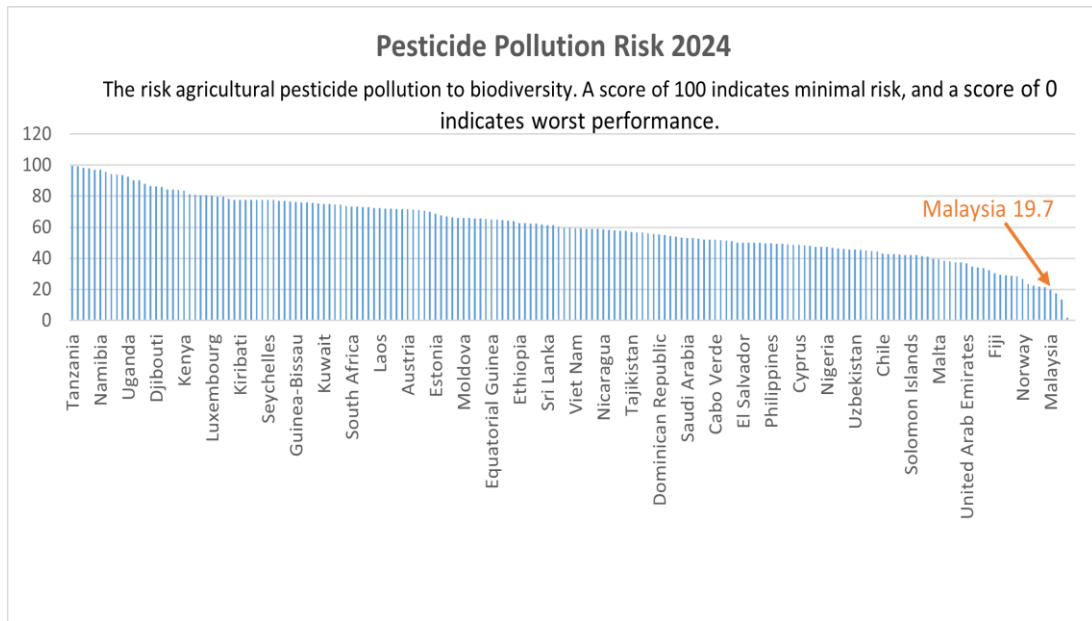


Figure 2.4 The Environmental Performance Index for pesticide pollution risk (2024) in 180 different countries (EPI, 2024).

### 2.2.2 Systematic classification of pesticides

Classifying pesticides based on characteristics aids in determining appropriate techniques and precautions (Alengebawy et al., 2021; Hassaan & El Nemr, 2020). One common classification divides them by origin into natural and synthetic types (Figure 2.5).

The various sub-categories of natural pesticides include:

- i. **Biochemical pesticides:** Employ natural substances like insect pheromones or plant extracts (e.g., geraniol) for pest control (Singh et al., 2015).
- ii. **Microbial pesticides:** Utilize microorganisms (bacteria, viruses, fungi) as active agents, often pest-specific (e.g., *Bacillus thuringiensis* (Bt) strains, Nuclear Polyhedrosis Virus (NPV)) (Kachhawa, 2017).
- iii. **Plant-based Pesticides:** Biocidal substances synthesized by plants, sometimes through genetic modification (e.g., BT crops producing Cry proteins), or derived from plant extracts/oils (Bharti et al., 2013).
- iv. **Mineral Oils:** Highly processed paraffinic oils used for pest control, sometimes effective against resistant strains (Nile et al., 2019).

Synthetic pesticides are subdivided based on active ingredients:

- i. **Inorganic Pesticides:** Include elements or salts like copper sulphate or sulphur; few remain in widespread use (Hassan, 2019).
- ii. **Organic Pesticides:** Classified by chemical structure and toxicological properties. Major groups include insecticides (e.g., organophosphorus (OPs), carbamates, pyrethroids), herbicides (e.g., bipyridyls, triazines), and fungicides (e.g., dithiocarbamates) (Alengebawy et al., 2021).

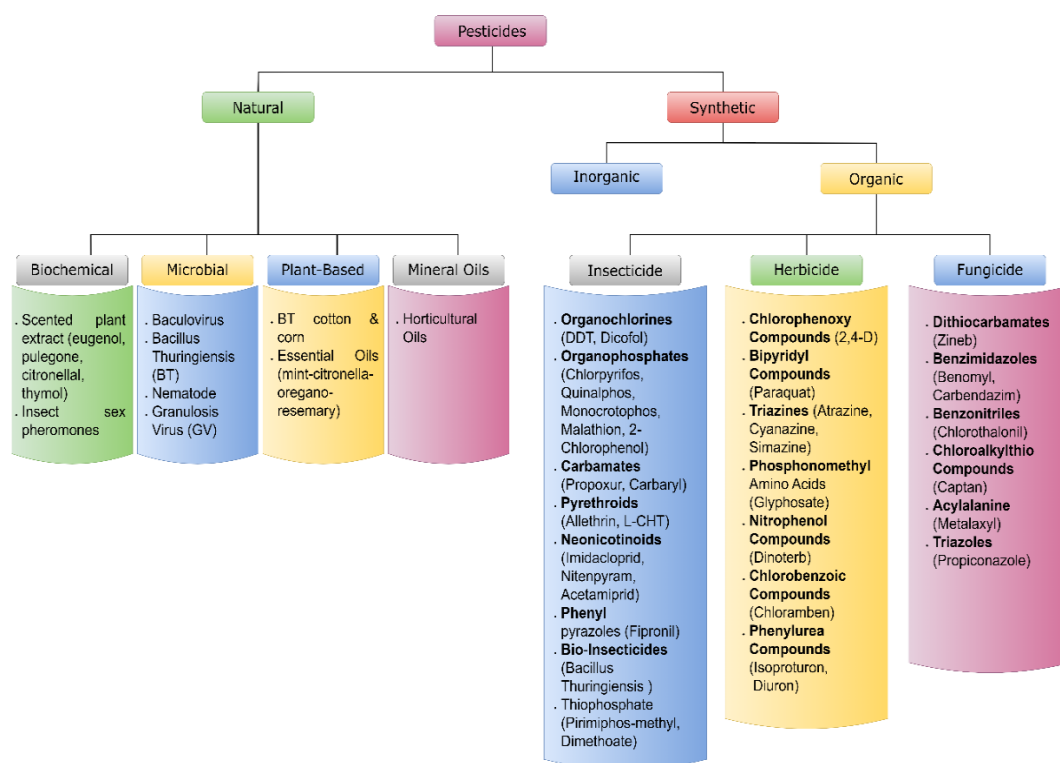


Figure 2.5 Classification of Pesticides (Ansari et al., 2021) (Hassaan & El Nemr, 2020) (Alengebawy et al., 2021)

The other form of pesticide classification is mentioned in Table 2.2, 2.3, 2.4 and 2.5. Also, Figure 2.6 demonstrates the chemical structure of a few common pesticides.

Table 2.2 Pesticide classification on the basis of commercial forms

Type of Pesticide	Description	Examples
Tablet	Pesticide presented in "pill" form	Aluminium phosphide
Dust	Pesticide in dry, finely powdered form	Boric acid, Sulfur
Liquid	Concentrated pesticide mixed with water for application	Roundup, Vantage
Dry Bait	Pesticide combined with edibles, forming dry pellets to attract pests	Klerat
Smokes	Pesticide mixed with combustible materials generating hot gas	Mosquito coil
Fumigants	Vaporous pesticides used in enclosed spaces to eliminate organisms	Cyanide, Aluminium phosphide, Methyl bromide

Table 2.2 (Continued)

<b>Type of Pesticide</b>	<b>Description</b>	<b>Examples</b>
Emulsion	Pesticide with one liquid dispersed as droplets in another, requiring agitation	Buctril
Wettable Powders	Crushed particles mixed with substances to form a water-suspendable powder	Blast-off
Granules	Larger dry particles of pesticides	Permetrol, Carbofuran

Source: (Ansari et al., 2021)

Table 2.3 Pesticide classification based on targeted pest species

<b>Type of Pesticide</b>	<b>Description</b>	<b>Examples</b>
Larvicides	Kills larvae	Lavimax
Algaecides	Kills algae	Argos
Nematicides	Kills nematodes (small worms feeding on plant roots)	Neemate-10G
Insect Repellents	Repels insects, e.g., citronella (essential oil)	Citronella (EO)
Rodenticides	Eliminates rodents (rats and mice)	Warfarin
Fungicides	Eliminates fungi	Captan
Insecticides	Used to kill insects	Neem, Carbamates
Pheromones	Disrupts mating behavior of insects to control them	-
Acaricides	Kills ticks	A-one
Herbicides	Kills weeds	Glyphosate
Ovicides	Kills insect and mite eggs	Hexygon DF
Bactericides	Kills bacteria	Carbolic acid
Molluscicides	Kills snails and slugs	Snailtox 70 WP
Miticides	Kills moths	Terro moth trap

Source: (Ansari et al., 2021)

Table 2.4 Pesticides classification on the basis of persistency

<b>Pesticide Persistence</b>	<b>Example Categories</b>	<b>Duration</b>
Highly Persistent	Organochlorines (dieldrin, DDT, aldrin)	Fifteen years or more
Intermediate	OPs (malathion, carbaryl, parathion)	Several months
Low Persistence	Carbamates (Tenik, Zectran, Zineb)	Around 2 weeks
Nonpersistent	Synthetic pyrethroids (cypermethrin, permethrin)	Short-lived

Source: (Ansari et al., 2021)

Table 2.5 Classification based on the World Health Organization's guidelines for pesticide toxicity (WHO).

<b>WHO Class</b>	<b>Toxicity Level</b>	<b>LD<sub>50</sub> for the Rat (mg/kg Body Weight)</b>		<b>Examples</b>
		<b>Oral</b>	<b>Dermal</b>	
Type Ia	Extremely hazardous	<5	<50	Parathion, Dieldrin
Type Ib	Highly Hazardous	5-50	50-200	Eldrin, Dichlorvos
Type II	Moderately hazardous	50-2000	200-2000	DDT, Chlordane
Type III	Slightly hazardous	>2000	>2000	Malathion

Source: (Ansari et al., 2021)

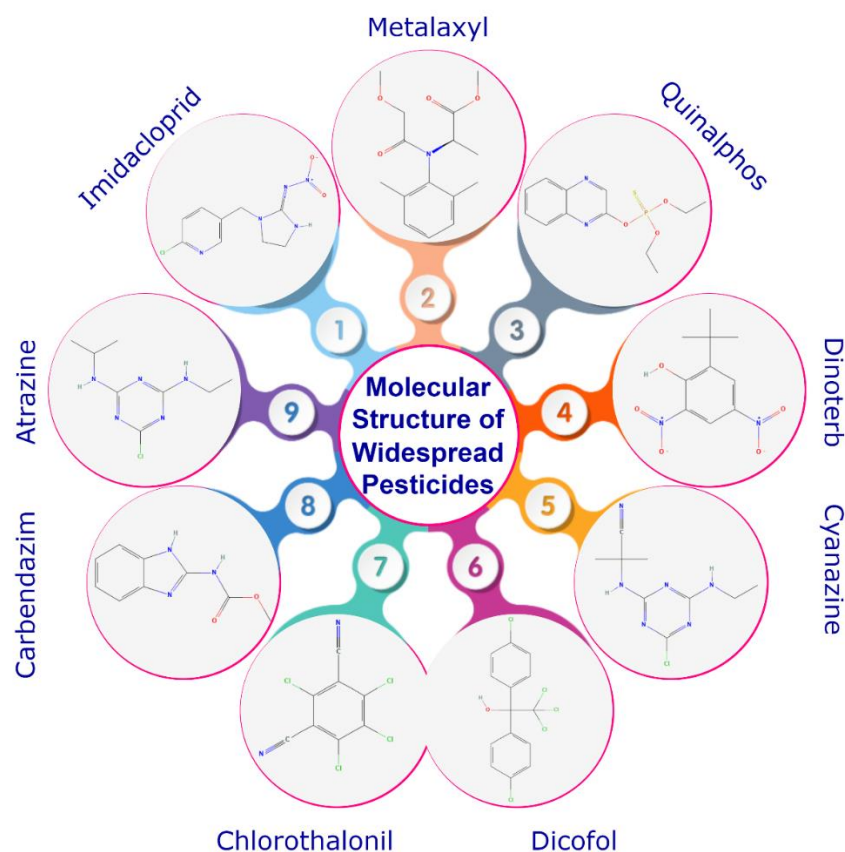


Figure 2.6 Molecular structures of most common pesticides.

### 2.3 Organic pollutant: Imidacloprid

Imidacloprid (IMD), a synthetic insecticide, also known as 1-[(6-chloro-3-pyridinyl) methyl]-N-nitro-2-imidazolidinimine (Figure 2.7), is the initial example of neonicotinoid insecticides (NEO-Is) and the most significant product in the market. (NEO-Is) have gained recognition as a type of pollutants that are widespread in surface water, ground water, and even drinking water. They can be detected at concentrations ranging from nanograms per litre (ng/L) to micrograms per litre ( $\mu\text{g/L}$ ) (Xue et al., 2023). Imidacloprid is a highly effective insecticide to control sucking insects. It has a wide range of activity, both by direct contact and systemic action. It effectively controls sucking insects through contact and systemic action by disrupting their central nervous system, similar to nicotine. IMD possesses a comparable chemical composition to nicotine and operates in a similar manner, impacting the central

nervous system of insects and ultimately resulting in paralysis and fatality (Garrido et al., 2024). Imidacloprid products have a dominant position in the insecticide market, being authorised for use in more than 120 countries and on over 140 different crops (Afridi & Umar, 2025).

Imidacloprid has the capacity to pollute surface water by its introduction into water bodies from crops, unintentional spills, or spray drift (Topal et al., 2017). While first believed to have negligible toxicity to non-target organisms, mounting data indicates that persistent exposure to imidacloprid may lead to possible consequences. IMD has been found to accumulate in soil, animals, and domestic water. According to a study, the level of IMD in agricultural water might reach up to 200 µg/L. Additionally, it has the ability to infiltrate lakes or rivers via runoff from the land and possesses a high level of toxicity against aquatic invertebrates (Raby et al., 2019). According to reports, the aerobic half-life of IMD can extend up to 997 days (Liang et al., 2022). The very resistant nature of this product is attributed to the stability and toxicity of the IMD (Čižmar et al., 2021; Akbari et al., 2022). Research has demonstrated that long-term exposure to imidacloprid resulted in lipid peroxidation and DNA damage in rainbow trout and earthworms (Wang et al., 2016). Furthermore, studies have demonstrated that imidacloprid can induce long-term harm to non-target aquatic arthropod species (Huang et al., 2022). Furthermore, imidacloprid has been shown in several studies to modify fish physiological processes, particularly in the embryo, resulting in lower viability and hatching success (Erhunmwunse et al., 2023). Additionally, imidacloprid has been connected to decreased hatching rates of fertilised eggs (Islam et al., 2019), oxidative stress, DNA damage (Vieira et al., 2018), and histological abnormalities in *Labeo rohita* tissues (Qadir & Iqbal, 2016).

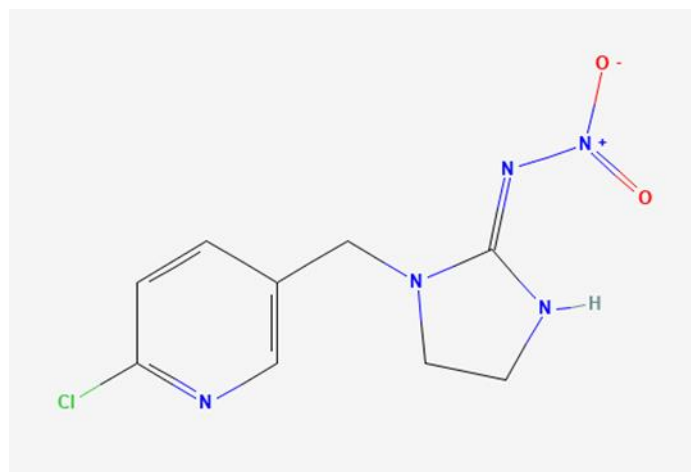


Figure 2.7 Chemical structure of Imidacloprid (IMD).

### 2.3.1 Previously reported photocatalysts for Imidacloprid degradation

A study using sonochemically exfoliated  $g\text{-C}_3\text{N}_4$  (CNS) found that the  $0.5\text{CNS}/\text{TiO}_2$  composite achieved 93% removal of 10 ppm IMD within 150 minutes under UV-Vis light irradiation (catalyst dose 1 g/L). This enhanced performance, compared to pristine components, was attributed to the formation of a heterojunction, which reduced the effective band gap and suppressed charge carrier recombination. The material demonstrated stability upon regeneration (Kobkeatthawin et al., 2022).

Another study reported  $\text{Ag}_2\text{O}/\text{CuO}$  composites synthesized via co-precipitation method as an excellent catalysts for the photocatalytic degradation of imidacloprid. The maximum degradation of imidacloprid was observed for  $10\text{ mg L}^{-1}$  imidacloprid solution with 0.01 g catalyst at pH 11 in the presence of UV light. The optimum temperature for the degradation process was found to be  $30\text{ }^\circ\text{C}$ . The results showed 92.3% degradation of imidacloprid in 180 minutes. The degradation followed first-order kinetics. The catalyst was able to be reused for up to 3 cycles with slight reduction in activity (Rashid Tariq et al., 2023).

Next, a 5% (w:w) silver doping in ZnO nanoparticles by a photo-reduction method was used as a photocatalyst for IMD degradation. The average nanoparticle size was 26.6 nm. The Ag doped ZnO achieved 45% degradation rate after 60 minutes of degradation whereas, only 30% degradation rate was achieved for pristine ZnO with 50 mg/L of ZnO load, 5.5 mg/L for imidacloprid initial concentration, 35°C for reaction temperature and it is 11 for the pH value (Atwan et al., 2019). Hence, silver doping on the ZnO surface may enhance the imidacloprid photo degradation.

Immobilizing ZnO nanoparticles within a calcium alginate matrix created a composite that combines adsorption and photocatalysis. This system achieved significant IMD degradation under simulated solar light (50% in 40 min, 80% in 2 hours, 94% in 3 hours). Performance was optimal under neutral to slightly basic conditions and influenced by the point of zero charge (pH<sub>zcp</sub>), as reported by Zyoud et al., (Zyoud et al., 2024).

Graphitic carbon nitride synthesized from urea demonstrated notable activity as a metal-free photocatalyst. It achieved approximately 90% degradation of IMD in 5 hours under visible light ( $\lambda > 400$  nm, 300W Xe lamp, 1 g/L catalyst). The precursor material was found to be important, with urea-derived g-C<sub>3</sub>N<sub>4</sub> being much more active than melamine-derived g-C<sub>3</sub>N<sub>4</sub> (42.9% efficiency) (Liu et al., 2015).

The Fe<sub>3</sub>O<sub>4</sub>/COF (Magnetic Covalent Organic Frameworks) were primarily investigated for IMD adsorption due to their high surface area (adsorption capacities 375-600 mg/g). However, these magnetic COFs (related porous polymers) also exhibited photocatalytic activity. Fe<sub>3</sub>O<sub>4</sub>/COF achieved 98.5% IMD degradation (10 mg/L initial conc., 0.01 g catalyst) in 5 hours under UV light at pH 11. The magnetic Fe<sub>3</sub>O<sub>4</sub> core facilitates easy separation and recovery (AlNeyadi et al., 2024).

Furthermore, perovskites, materials with a characteristic  $ABX_3$  crystal structure (often oxides  $ABO_3$ ), are gaining attention in photocatalysis due to their tunable band gaps, compositional flexibility allowing property optimization, and generally good stability. One such photocatalyst system of  $Co_3O_4$ - $MoO_3$  composites which achieved ~98% IMD degradation in 150 min under natural sunlight by significantly reducing the band gap (from 2.88 eV to 2.15 eV), demonstrates the viability of using complex oxide structures for visible-light-driven IMD removal (Adam et al., 2023).

A composite using thiol-functionalized Carbon Quantum Dots (CQDs-SH) to passivate (stabilize) Cadmium Sulfide (CdS) Quantum Dots achieved 90.1% IMD degradation in 90 minutes under simulated visible light at pH 9. This highlights the use of quantum dots. Also, the results of this study demonstrated a strong role of pH in determining degradation outcomes (Targhan et al., 2024).

A ternary composite involving polyaniline (PANI), tungsten trioxide ( $WO_3$ ), and cadmium sulfide (CdS) reportedly degraded 94.7% of 10 ppm IMI at pH 3. This combines a conducting polymer with two different semiconductors, likely forming complex heterojunctions. Related  $WO_3@PANI$  composites were effective for dye degradation (Merci et al., 2021). A summary of these studies is tabulated in Table 2.6.

Table 2.6 Summary of key studies on photocatalytic degradation of Imidacloprid using nanocomposites.

Nanocomposite Type	Degradation Efficiency (%)	Time (min)	Initial IMD Conc. (mg/L)	Light Source	Ref.
g-C <sub>3</sub> N <sub>4</sub> /TiO <sub>2</sub> (0.5CNS)	93	150	10	UV-Vis	(Kobkeatthawin et al., 2022)
Co <sub>3</sub> O <sub>4</sub> -MoO <sub>3</sub>	98	150	15	Visible	(Adam et al., 2023)
ZnO@Ca-Alginate	94	180	N/A	Sim. Solar	(Zyoud et al., 2024).
g-C <sub>3</sub> N <sub>4</sub> (Urea-derived)	~90	300	N/A	Xenon Lamp	(Liu et al., 2015)
Fe <sub>3</sub> O <sub>4</sub> /COF	98.5	300	10	UV	(AlNeyadi et al., 2024)
CQDs-SH/CdS QDs	90.1	90	N/A	Sim. Visible	(Targhan et al., 2024)
PANI/WO <sub>3</sub> -CdS	94.7	N/A	10	N/A	(Merci et al., 2021)
Ag <sub>2</sub> O/CuO (5%)	92.3	180	10	UV	(Rashid Tariq et al., 2023)
Ag(5%)-ZnO	45	60	5.5	Day light	(Atwan et al., 2019)
GO/ZnO/Ag (This study)	100	135	25	UV-Visible	

## 2.4 Various bio precursors for graphene derivatives synthesis

### 2.4.1 Rice Husk

Annually producing around 120 million tonnes, rice husk is an abundant biomass source rich in cellulose and lignin, making it suitable for graphene production via various methods. Rice husk enables the production of graphene using both top-down and bottom-up methods. Rice husk is an excellent choice due to its potential for widespread graphene manufacturing (Wang et al., 2016).